THE EFFECT OF SERIES ELASTICITY ON THE FORCE-LENGTH RELATIONSHIP OF SKELETAL MUSCLE

By Brian Hamilton

A Thesis

Submitted in Partial Fulfillment

of the Requirements for the Degree of

Master of Science
in Biology

Northern Arizona University

May 2023

Approved:

Natalie C. Holt, Ph.D., Chair

Kiisa Nishikawa, Ph.D.

Timothy Becker, Ph.D.

ABSTRACT

THE EFFECT OF SERIES ELASTICITY
ON THE FORCE-LENGTH RELATIONSHIP
OF SKELETAL MUSCLE

Brian Hamilton

Skeletal muscle contains molecular motors that allow for voluntary movement in vertebrate organisms. It has been widely accepted that skeletal muscle has a narrow range of operating lengths that provide peak force and that this force-length relationship is dictated by the amount of overlap of thick and thin myofilaments. However, much remains unknown about the molecular mechanics of skeletal muscle. This is especially true in dynamic movement, where the isometric force-length relationship tends to fall short in accurately predicting optimum length, the length at which peak force is produced. When attempting to predict *in* vivo muscle behavior with the isometric force-length relationship, systematic errors may occur due to varying activation levels, active length changes, and lack of structural homogeneity between organisms and within an organism. To elucidate a potential mechanism for observed experimental shifts in optimum length with varying activation levels, experiments were performed on muscles with parallel fiber orientation that were sutured to an external in-series artificial elastic component with considerable compliance. These muscles were attached to a stationary clamp on one side and a force-measuring ergometer on the other. Maximal contractions were elicited at a wide range of starting lengths both with and without the artificial tendon and force-length graphs were constructed. Optimum length with an artificial tendon and resultant shortening decreases to approximately 89.26 ± 5.21% compared to the optimum length of purely isometric contractions. This lends support to the hypothesis that a purely mechanical mechanism driven by shortening may be responsible for the majority of the shifts in optimum length and that, similar to observations in experiments with varying activation levels, this shift may not be driven solely by the length dependence of calcium sensitivity.

ACKNOWLEDGEMENTS

I would like to thank Dr. Natalie Holt for her support, guidance, and unwavering patience through every obstacle that arose. I would also like to thank Drs. Dave Williams, Kiisa Nishikawa, and Tim Becker for insightful discussions. Additionally, I am grateful to undergraduate researchers Carmella Brown and Victoria Deyoung for their willingness to help with some of the more challenging aspects of this project. Special thank you to NAU and UCR for providing start-up funds.

Brian Hamilton[1], Carmella Brown[1], Victoria Deyoung[1], Natalie C. Holt[2]

[1]Department of Biological Sciences, Northern Arizona University, 1899 S San Francisco St, Flagstaff, AZ 86011

[2]Department of Evolution, Ecology, and Organismal Biology, University of California, Riverside, Eucalyptus Dr #2710, Riverside, CA 92521

Email: bh558@nau.edu

TABLE OF CONTENTS

INTRODUCTION

Muscle Structure

In vertebrate organisms, voluntary movement is generated by skeletal muscle. From large to small-scale structures, skeletal muscle is composed of muscle fascicles making up a whole muscle, muscle fibers making up a fascicle, and myofibrils making up a muscle fiber or cell. Muscles are attached to bone by fibrous connective tissue sheets known as aponeuroses, and tendons. Tendons provide passive elastic tissue that conserves energy and protects muscles (Cavagna et al., 1964; Holt, Roberts, et al., 2014; Roberts, 2016), while muscles contain the molecular motors that actively generate force for movement.

Skeletal muscle is made up of a complex arrangement of proteins that give them their striated appearance. Myofibrils are composed of thick and thin filamentous contractile proteins. Thin filaments are primarily composed of actin and the regulatory proteins troponin and tropomyosin, and thick filaments are primarily composed of myosin. Contractile proteins are arranged longitudinally to form contractile units called sarcomeres (**Figure 1**). Sarcomeres and myofilaments within them give skeletal muscle its striated appearance at the microscopic level (**Figure 1a**). The I-band, which is primarily composed of thin filaments, appears as the lighter bands, while the dark A-bands are composed of the thick filaments and the regions of overlap between the thick and thin filaments (**Figures 1a & 1b**). Sarcomeres terminate on Z-disks, and sarcomere lengths can be measured by the distance between neighboring Z-disks (Huxley, 1957; Huxley & Niedergerke, 1954). When muscles contract, a complex series of events occurs that results in changes in the appearance of muscle sarcomeres. This series of events starts with excitation-contraction coupling (Sandow, 1952).

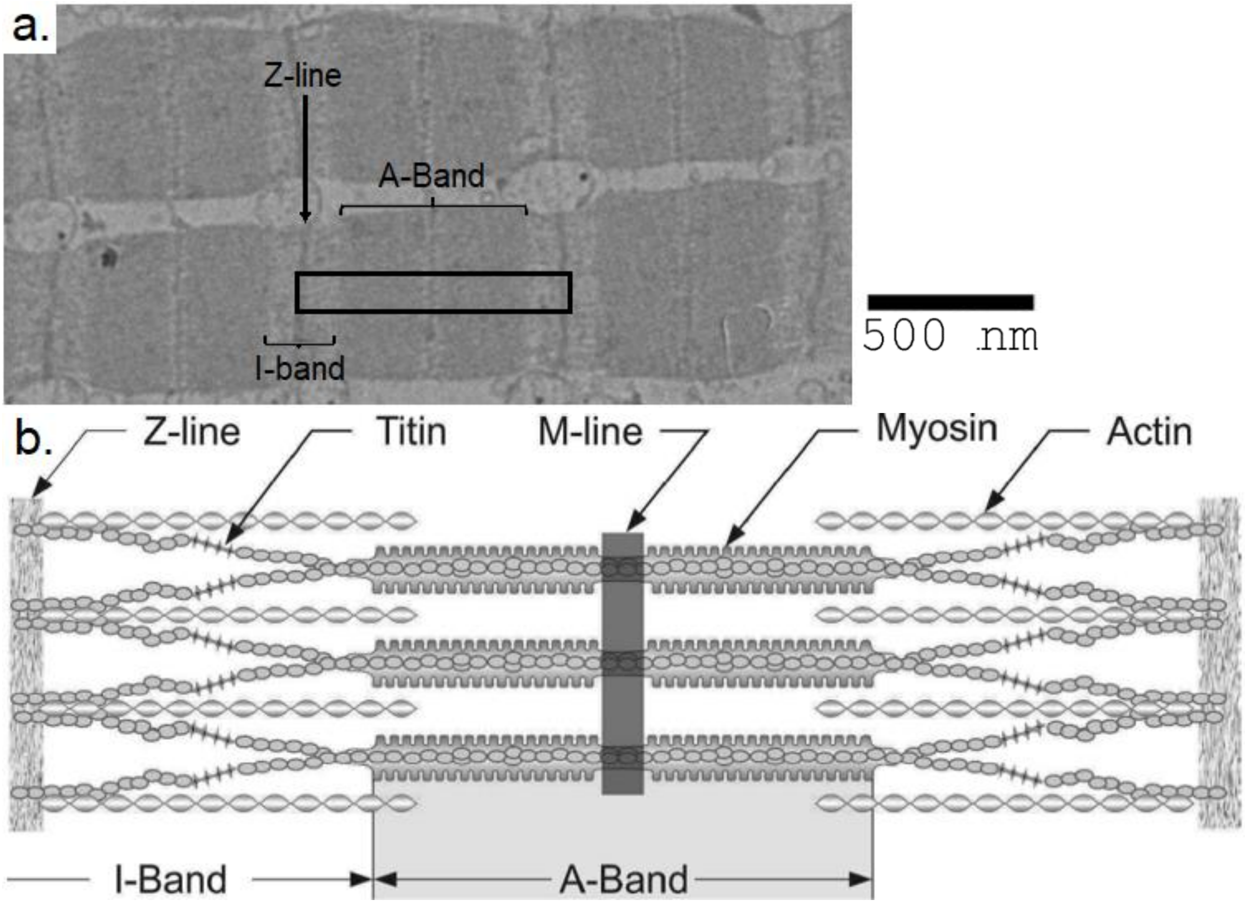

Figure 1. Transmission electron micrograph of myofibrils (a) and diagram of the rectangular cutout showing structural landmarks within a sarcomere (b) (Figure 1a imaged at Northern Arizona University Imaging Histology Core Facility; Figure 1b adapted from Granzier & Labeit, 2006; J. A. Herzog et al., 2014).

Excitation-Contraction Coupling

In response to activation by the nervous system, excitation-contraction coupling (ECC) begins when neurotransmitters are released from a motor neuron and bind to receptors in the sarcolemma of a muscle fiber, causing a transmembrane potential change called a motor unit action potential (MUAP; Randall et al., 1997). A transverse tubule system carries the MUAP deep within the muscle fiber and causes a conformational change in calcium channels in the sarcoplasmic reticulum (SR), the calcium storage area in striated muscle cells, which stimulates the release of calcium into the sarcoplasm of the muscle fiber. The regulatory protein tropomyosin blocks myosin binding sites on actin until calcium enters the sarcoplasm. Once calcium diffuses into the sarcoplasm, it binds to troponin, which undergoes a conformational change that causes tropomyosin to reveal binding sites on actin. Myosin heads then bind to actin, forming cross-bridges, and undergo a force-generating conformational change known as a powerstroke, before detaching from actin. These force-producing interactions occur until MUAPs cease, at which point calcium is pumped back into the SR and muscle relaxation takes place. At the whole-muscle level, the amount of force produced by ECC and subsequent force-producing interactions between actin and myosin varies depending on the level of muscle activation (Adrian & Bronk, 1929; Liddell & Sherrington, 1925).

Muscle Activation

During movement, activation levels change to meet the demands of the activity being performed and muscles are rarely, if ever, maximally activated (Hodson-Tole & Wakeling, 2009; Holt, Wakeling, et al., 2014; Strojnik, 1995). Activation levels can be modulated in two ways: by varying the frequency of motor neuron action potentials, also known as rate coding (Adrian & Bronk, 1929), and by varying the number of motor units recruited (Liddell & Sherrington, 1925).

Rate coding is a change in muscle activation that is achieved by changing the frequency of action potentials delivered to muscle fibers. As action potential frequency increases, calcium concentration within individual muscle fibers increases and is accompanied by a graded increase in force until maximum force is reached (Adrian & Bronk, 1929; Brown et al., 1999). The amount of isometric force produced at a given calcium concentration is thought to be related to the proportion of troponin molecules that have calcium bound and have caused a conformational change in tropomyosin, allowing cross-bridges to be formed (Rassier et al., 1999). Since changing action potential frequency causes a change in intracellular calcium concentration, rate coding is a calcium-dependent mechanism of force production.

A motor unit is a motor neuron and all of the muscle fibers it innervates. According to the size principle, slow motor units with slower twitch, smaller diameter muscle fibers are recruited first and fast motor units with fast twitch, larger diameter muscle fibers are recruited as demand increases (Henneman, 1957; Henneman et al., 1965). Changing motor unit recruitment is a calcium-independent process since the calcium concentration in active muscle fibers recruited is expected to be approximately the same provided rate coding is the same. Muscle contraction during movement likely involves a combination of varying both rate coding and motor unit recruitment. Once activated by the process of excitation contraction coupling, muscle force has been proposed to develop according to the cross-bridge and sliding filament theories of contraction (Huxley, 1957, 1974; Huxley & Niedergerke, 1954; Huxley, 1969; Huxley & Hanson, 1954).

Cross-bridge and sliding filament theories

The sliding filament theory states that actin and myosin slide past one another and shorten the sarcomere during concentric muscle contraction (Huxley, 1974; Huxley & Niedergerke, 1954; Huxley, 1969; Huxley & Hanson, 1954). This theory was formed by observation of the changing appearance of muscle striations at different muscle lengths. At shorter lengths, Z-disks are closer together and there is more actin-myosin overlap than at longer lengths, as supported by the decrease in the width of the I-band. As a muscle lengthens and Z-disks move farther apart, the A-band remains unchanged and there is an increase in the width of the I-band, supporting the inference that actin-myosin overlap decreases as sarcomeres are stretched. The cross-bridge theory offers an explanation for the molecular mechanics behind the sliding filament theory (Huxley, 1957). It states that the cyclical process of actin-myosin cross-bridge formation, power stroke, and detachment during muscle contraction moves neighboring Z-disks closer together.

This understanding of sarcomere mechanics confers fundamental properties of muscle including the force-length and force-velocity relationships (Gordon et al., 1966; Hill, 1938; Huxley & Simmons, 1971).

Force-length relationship

According to the classic force-length relationship, skeletal muscle has a narrow range of optimum lengths at which it produces peak force under maximally activated, isometric conditions (**Figure 2**). The force-length relationship states that peak isometric force is produced at an intermediate muscle length, where overlap of actin and myosin is optimal and the most force-producing cross-bridges can be formed (Gordon et al., 1966; Herzog et al., 2010). As muscle length increases beyond optimal length, actin-myosin overlap decreases and fewer force-producing cross-bridges can be formed, causing the force to decrease on the descending limb. Though the ascending limb was thought result from thin filaments colliding with the Z-disk (Gordon et al., 1966), more recent work has shown that it may be due to changes in the interfilament spacing as sarcomeres reach short lengths (Bagni et al., 1990; MacIntosh, 2017; Rockenfeller et al., 2022). However, other findings suggest that lattice spacing may not be responsible for the majority of the decrease in force on the ascending limb in relaxed, skinned fibers (Konhilas et al., 2002).

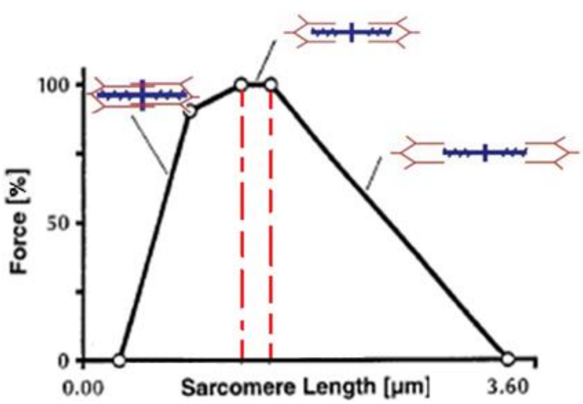

Figure 2. Muscle force-length relationship and sarcomere length (adapted from Gordon et al., 1966).

Force-velocity relationship

According to the force-velocity relationship, the force a muscle can produce declines with increasing velocity during shortening (Hill, 1938). This is thought to be due to the limited time available for cross-bridges to generate force and detach during rapid shortening **(Figure 3)**. It is important to note that the experiments behind the discovery of the force-length and force-velocity relationships were performed under tightly controlled, maximally activated conditions that may not be representative of *in vivo* dynamic movements like running and walking. During such movements, muscles experience varying activation and undergo complex patterns of length change.

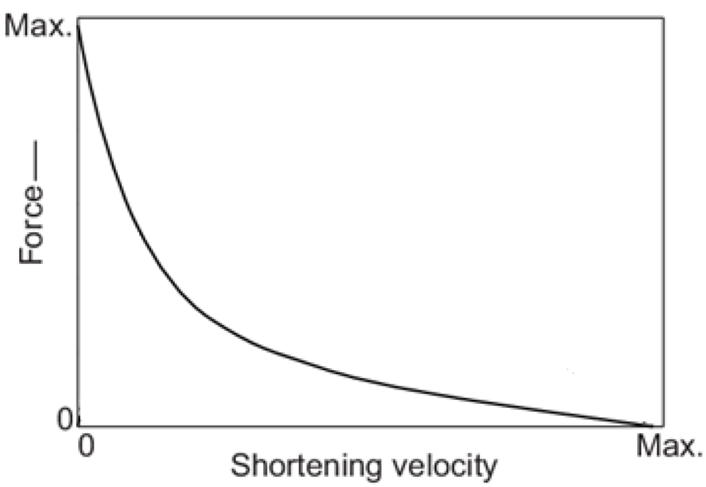

Figure 3. The magnitude of force that a muscle can produce decreases as shortening velocity increases (from Lindstedt, 2016; adapted from Hill, 1950)

Challenges to the early theories of muscle contraction

The cross-bridge and sliding filament theories offer an explanation for the molecular mechanics of muscle contraction and have been used to develop Hill-type muscle models that predict muscle force as a function of activation state, force-length, and force-velocity properties (Winters, 1990; Zajac, 1989). These theories and Hill-type muscle models have been widely used to explain and predict muscle performance (Hutchinson et al., 2015; O'Neill et al., 2013).

However, the accuracy of the early theories and Hill-type muscle models in predicting muscle force production in physiologically relevant conditions like running and walking *in vivo* is largely unknown, and discrepancies between predicted and measured forces have been documented (Dick et al., 2017; Perreault et al., 2003). There are many potential reasons for these discrepancies. For example, a third filamentous muscle protein, titin, spans the length of the sarcomere and affects both the passive and active mechanics of muscle contraction (Duvall et al., 2013; Joumaa et al., 2008; Labeit et al., 2003; Nishikawa et al., 2012). In addition, the thick and thin filaments themselves are more complex than assumed by the cross-bridge and sliding filament theories, exhibiting some degree of compliance and so deforming slightly during contraction (Goldman & Huxley, 1994; Huxley et al., 1994; Wakabayashi et al., 1994).

Some of the complex features of muscle have been suggested to be responsible for other phenomena related to history-dependent effects that occur after active changes in length. For example, force enhancement is an increase in force at a given length following an active muscle stretch compared to purely isometric contractions (Abbott & Aubert, 1952; Edman et al., 1982; W. Herzog et al., 2006; Nishikawa, 2016). Conversely, force depression is the reduction of force after active muscle shortening compared to purely isometric contractions (Abbott & Aubert, 1952; Rassier & Herzog, 2004). There are also changes in the force-length relationship with changing activation levels (Abbott & Aubert, 1952; Edman et al., 1982; Herzog et al., 2006; Holt & Azizi, 2014; Minozzo & de Lira, 2013; Nishikawa, 2016; Rack & Westbury, 1969; Rassier & Herzog, 2004). Certain aspects of these phenomena cannot be explained by the cross-bridge or sliding filament theories.

Activation-dependent changes to the force-length relationship

Basic properties of skeletal muscle are not consistent across activation levels (Holt et al., 2014; Rack & Westbury, 1969; Rassier & Herzog, 2004). Changing muscle activation causes non-linear changes in the force-length and force-velocity relationships compared to maximally activated, isometric contractions (Brown et al., 1999; Holt, Wakeling, et al., 2014; Holt & Azizi, 2014; Rack & Westbury, 1969). Among these changes is the shift in L_0 with activation level (Holt & Azizi, 2014; Holt & Williams, 2018; Rack & Westbury, 1969; Rassier et al., 1999). However, the cause of this shift is unclear. Length dependence of calcium sensitivity has been proposed, suggesting that muscle fibers are more sensitive to calcium at longer lengths (Stephenson & Wendt, 1984), possibly due to changes in intermyofilament spacing in a shortening isovolumetric muscle (Fuchs & Smith, 2001; MacIntosh, 2017; Rassier et al., 1999; Yang et al., 1998). Although there almost certainly is some effect of length-dependence of calcium sensitivity on L_0, this effect is likely to be small (Holt & Azizi, 2014; Holt & Williams, 2018).

Rather than changes in calcium sensitivity, absolute force may be responsible for changes in L_0 at different activation levels when additional in-series compliance is present (Holt & Azizi, 2014; Holt & Williams, 2018). In bullfrog plantaris muscles, a large activation-dependent shift in L_0 has been observed (Holt & Azizi, 2014). However, since this shift in L_0 was observed regardless of whether activation was varied by changing action potential frequency or by changing motor unit recruitment, it was concluded that length dependence of calcium sensitivity was not entirely responsible (Holt & Azizi, 2014; Holt & Williams, 2018). Since this shift was observed in the absence of calcium-based effects and the magnitude of shortening before isometry was proportional to the change in L_0, this suggests that some purely mechanical aspect of contractile history is responsible. This muscle has a large elastic tendon, and so it was proposed that shortening against this tendon might contribute to this shift in optimum length, and therefore that this shift may somehow be related to shortening depression (Holt & Azizi, 2014; Holt & Williams, 2018).

Here, I test this hypothesis by examining the effect of adding an artificial tendon to a muscle and determining the effect on the force-length relationship. I hypothesized that when an artificial tendon is mounted in-series with a bullfrog sartorius muscle, and the muscle is maximally activated, a decrease in L_0 would occur compared to maximal contractions without tendon due to an increase in shortening. I also predicted that peak force would be reduced due to shortening depression since the muscle actively shortens before reaching isometry.

METHODS

Experiments were performed on adult bullfrogs (*Rana [Lithobates] catesbeiana*). Subjects were purchased commercially and housed in a glass aquarium with access to water deep enough for swimming. Animals were housed and all work was performed with the approval of the Northern Arizona University Animal Care and Use Committee. Experiments were performed on the sartorius, a proximal hindlimb muscle which is largely parallel fibered and has minimal terminal tendons (Kargo & Rome, 2002). This choice of muscle meant that our artificial tendon contributed most of the series compliance outside of the muscle fibers. Subjects were euthanized by double-pithing. Sartorius muscles were excised and bathed in an oxygenated isotonic Ringer's solution (112 mM NaCl, 2.5 mM $CaCl_2$, 1mM $MgCl_2$, 3.3 mM KCl, 5 mM D-glucose, 20 mM HEPES; adjusted to pH 7.4 at room temperature using NaOH; Mayfield et al., 2016). Muscles were sutured in-series to an artificial tendon (Theraband; Akron, OH) using silk suture (5-0, Sharepoint; Reading, PA, USA) and mounted to an ergometer (series 305C-LR, Aurora Scientific Inc.; Ontario, Canada) that measured muscle force and length (**Figures 4 & 5**).

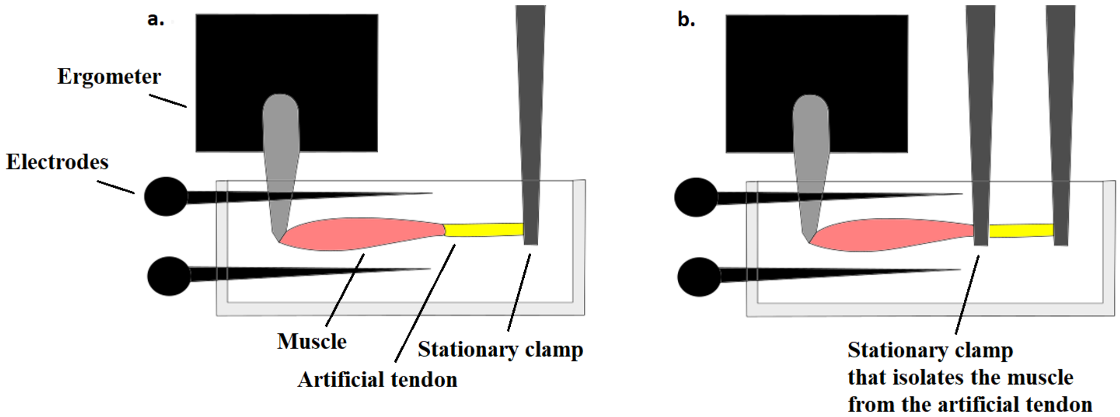

Figure 4. Schematic showing "w/ tendon" (a) and "muscle only" (b) conditions. In both conditions, MTU or muscle is attached to an ergometer on the left and static anchor on the right. In the "muscle only" condition, an additional stationary clamp is used to isolate the muscle from the artificial tendon. Muscle is submerged in isotonic Ringer's solution and is surrounded by electrodes that deliver stimulation.

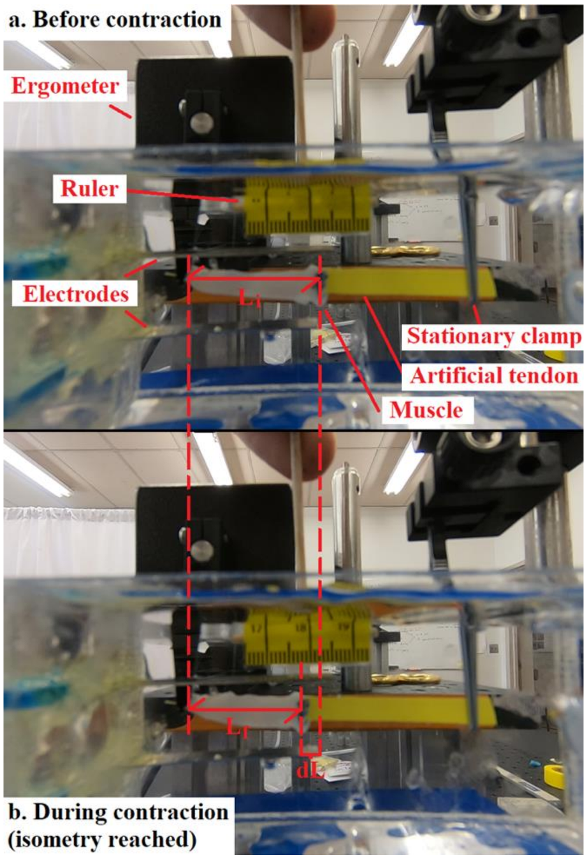

Figure 5. An example "w/ tendon" contraction. The top photo (a) shows the muscle before activation at its initial length (L_i). The lower photo (b) shows the active muscle at its shortened length (L_f) where isometry is reached. The amount of shortening is shown as the change in length (dL).

Fixed-end contractions were performed on each muscle by securing the muscle and tendon ends to stationary anchor clips in the "w/ tendon" condition and by inserting a stationary anchor clamp at the muscle end that excluded the tendon in the "muscle only" condition (**Figures 4 & 5**). Stimulation voltage for maximal tetanic contraction was found for each muscle by performing a series of twitch contractions at a range of voltages and the voltage that induced maximum twitch force, generally between 40 to 60 volts, was used to stimulate muscles tetanically with 0.2 ms square wave pulses at 100 Hz for 400 ms using platinum plate electrodes mounted above and below the muscle (S48, Grass; West Warwick, RI, USA). Muscles were stimulated at different starting lengths sufficient to construct a force-length curve both with and without the artificial tendon included. Contractions performed on muscles with the artificial tendon in-series were called the "w/ tendon" condition. The muscles shortened by approximately 15% of their initial length before reaching isometry. Contractions performed on muscles without the tendon contracted isometrically and were called the "muscle only" condition.

Muscle lengths for the "muscle only" condition and force for both conditions were recorded at 5000 Hz using a multifunction data acquisition board (USB-6212, National Instruments Corp.; Austin, TX, USA) and data analysis software (Igor Pro 7.0.8.1, Wavemetrics Inc.; Lake Oswego, OR, USA). To track muscle lengths and changes in muscle lengths for the "w/ tendon" condition, muscle contractions were video recorded (GoPro Hero 5 Black, GoPro Inc.; San Mateo, CA, USA). For each "w/ tendon" contraction and for several "muscle only" contractions, a ruler was submerged and placed just above the muscle for calibration, allowing conversion of muscle lengths from pixels to millimeters (ImageJ 1.52a, NIH; Rockville, MD, USA; see **Figure 5**). For "w/ tendon" contractions, muscle length changes were carefully restricted to a single plane and muscle length was tracked frame-by-frame using video analysis software (DLTdv7 extension, MATLAB R2018b, The MathWorks Inc.; Natick, MA, USA). Muscle shortening was calculated as the difference between initial length (L_0) and the final length (L_f) after the muscle reached isometry (**Figure 5**). Maximum shortening velocities for "w/ tendon" contractions that resulted in L_0 were found using the slope of the length curve in the initial shortening phase (**Figure 6**).

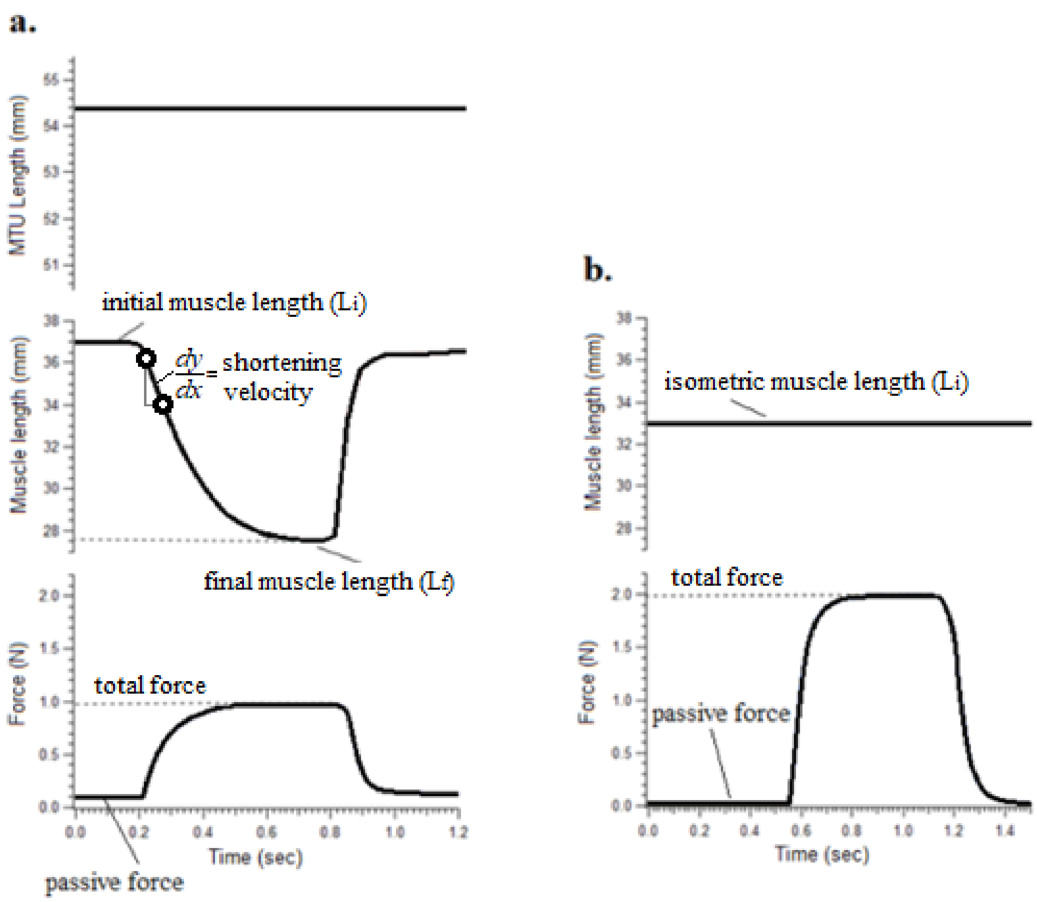

Figure 6. "W/ tendon" (a) and "muscle only" (b) force and length traces for one contraction of each type. Dashed lines represent the total force and length values that were gathered at isometry. Total force and passive force values were used to find active force, and active force and length values were used to construct a force-length curve (**Figure 7**; open points). Maximum shortening velocity was calculated using the slope between two points on the muscle length vs time trace in the "w/ tendon" condition.

Each muscle was stimulated at various initial lengths both with and without the artificial tendon. In the "w/ tendon" condition, muscles shortened against the in-series elastic band until they reached isometry. Length and force values were recorded for each contraction (**Figure 6**). In the "muscle only" condition, muscle length (L_{iso}) did not change. The starting condition ("w/

tendon" or "muscle only") and initial lengths were randomized. Peak shortening velocity was found by taking the steepest part of the muscle length vs time trace and calculating its slope (**Figure 6**). Peak shortening velocity was later used to analyze whether shortening velocity affects peak force.

Data Analysis

Force and length analysis and graph generation was performed in Igor Pro (**Figures 6 & 7**). Force and length time-series plots were constructed for each contraction and ergometer and video data were time-synchronized to align force and length changes. Total force for both the "w/ tendon" and "muscle only" conditions was the average of the force produced at isometry (Force (N) panels, **Figure 6**). Passive force for the "muscle only" condition was found by taking the average force value before muscle activation. Passive force was subtracted from total force to find active force for the "muscle only" condition. Once initial and final lengths were determined, passive force, active force, and final lengths for each contraction were used to construct active and passive force-length curves for the "muscle only" condition. Data were fit with a third-order polynomial (Holt & Azizi, 2014; **Figure 7**). Passive force curves for the "w/ tendon" condition were created using passive force data from the "muscle only" contractions and fit using an exponential function. These data were then extrapolated to the shorter lengths achieved in the "w/ tendon" condition after shortening (dashed grey line; **Figure 7**). Passive force was subtracted from total force to find active force in the "w/ tendon" condition. The peak force (P_0) and L_0 were determined from active "muscle only" and "w/tendon" force-length curves (**Figure 7**). The "w/ tendon" P_0 and L_0 values were converted to relative proportions of "muscle only" values using the following equation (**Equation 1**).

$$\text{Equation 1: } Proportion\ of\ L_{0\text{ “}muscle\ only\text{”}} = \left(\frac{L_0}{L_{0\text{ “muscle only”}}}\right)$$

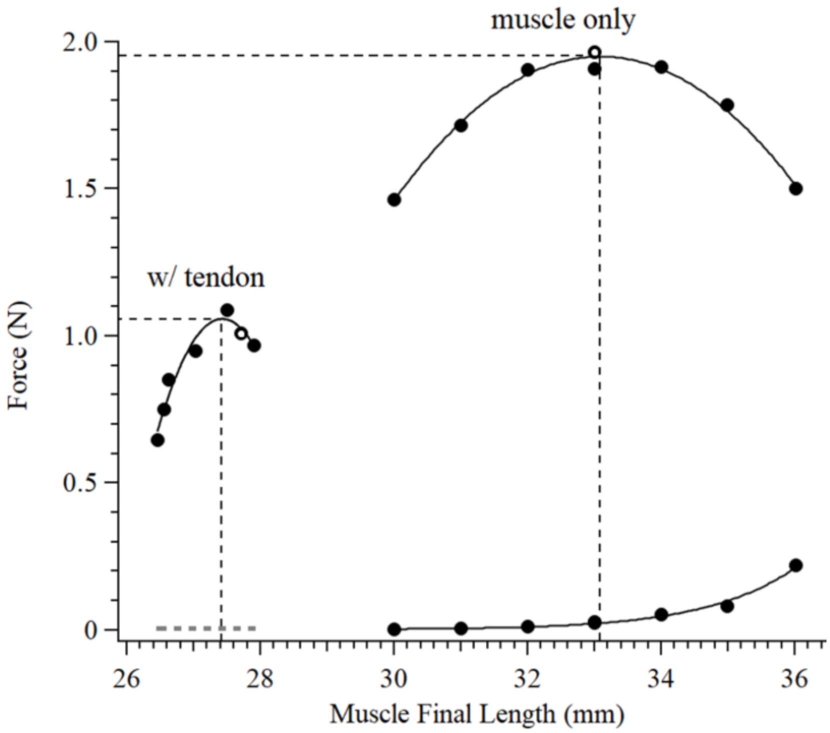

Figure 7. Force-length summary traces for “w/ tendon” and “muscle only” contractions on the same muscle. Upper curves labeled “w/ tendon” and “muscle only” are active force at isometry, lower curves are passive force pre-contraction. Dashed vertical and horizontal lines leading to peaks of each curve represent L_0 and P_0 values. The “muscle only” passive force was extrapolated to the “w/ tendon” shortened lengths (dashed grey line). Open points are the values from the force-length traces in **Figure 6**.

Statistical Analysis

A paired t-test was used to test whether there were significant changes in P_0 and L_0 as a result of adding an artificial tendon (R Studio; Boston, MA, USA). Since our sample size was small (n = 6), a Shapiro-Wilk test was used to check the normality of the distribution of the data.

RESULTS

The following values are expressed as mean ± s.e.m. The mean bullfrog mass was 104.40 ± 9.58 g and the mean sartorius muscle mass was 0.24 ± 0.04 g. Artificial tendon lengths were 15.4 ± 1.59 mm. Peak isometric stress (S_0) for the ”muscle only” condition was 19.95 ± 1.90 N/cm^2, which is similar to previously published S_0 values for frog sartorius muscles (Close, 1972).

There was a significant effect of adding additional series compliance on both P_0 ($p < 0.001$; paired t-test) and L_0 ($p < 0.01$; paired t-test). P_0 was 1.58 ± 0.27 N in the “muscle only” condition and 0.92 ± 0.13 N in the “w/ tendon” condition. Relative to “muscle only” values, the “w/ tendon” condition L_0 was 0.892 ± 0.052 and P_0 was 0.590 ± 0.085 (**Figure 8**). Though plateaus in the force-length curves were reached in both the “w/ tendon” and “muscle only” condition, substantial descending limbs were not achieved in the “w/ tendon” condition (**Figure 7**). For the “w/ tendon” contractions, L_i that resulted in L_0 was 30.44 ± 2.03 mm. Contractions that resulted in L_0 actively shortened 20.72 ± 5.39% of their initial lengths. The results of the Shapiro-Wilk test showed that the distribution of P_0 and L_0 were not significantly different from normally distributed ($p = 0.1153$). Maximum shortening velocity for contractions that resulted in L_0 was 38.12 mm/s ± 12.53 mm/s, which is greater than the average maximum shortening velocity for all contractions, 32.72 ± 12.90 mm/s. The amount of work performed for contractions that resulted in L_0 was 5.97 ± 2.44 mJ.

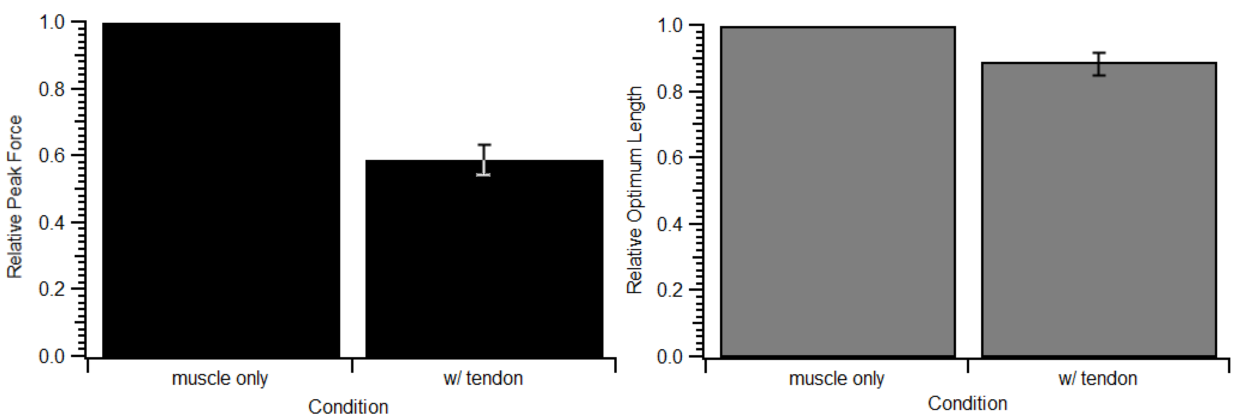

Figure 8. The “w/ tendon” condition decreased P_0 and L_0 compared to muscle only contractions. Relative values are calculated as the average peak force value divided by “muscle only” peak force value ± SD.

To see whether muscle shortening varied with different initial muscle lengths, an initial muscle length vs muscle shortening trace was constructed (**Figure 9**). There was a non-linear change in shortening as L_i increased (dashed vertical line, **Figure 9**). Similarly, an initial muscle length vs shortening velocity trace was constructed (**Figure 10**) to see if shortening velocity changed with different starting lengths. There was a non-linear change in shortening velocity as L_i changed, with peak shortening velocity occurring at intermediate lengths and decreasing as L_i increased or decreased. The data also showed that the highest shortening velocities occurred very near L_0 (dashed vertical line, **Figure 10**).

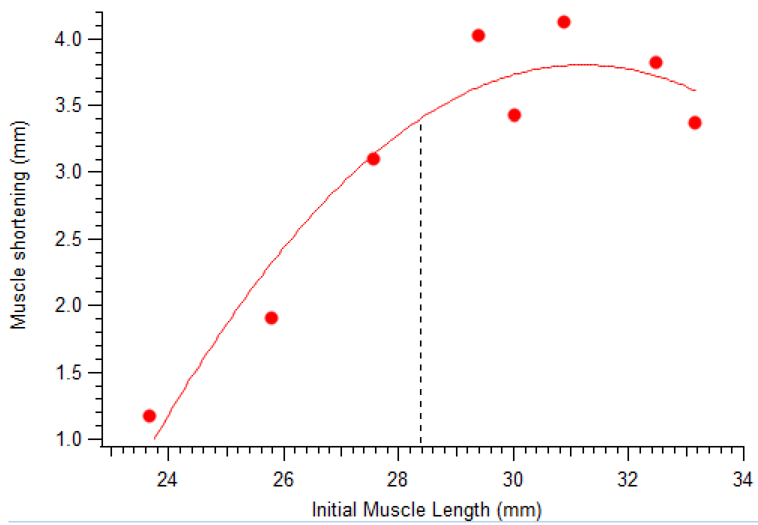

Figure 9. Graph showing the relationship between the amount of muscle shortening and the initial muscle length (before the muscle was contracted) for one muscle. Dashed line represents L_0 for this muscle.

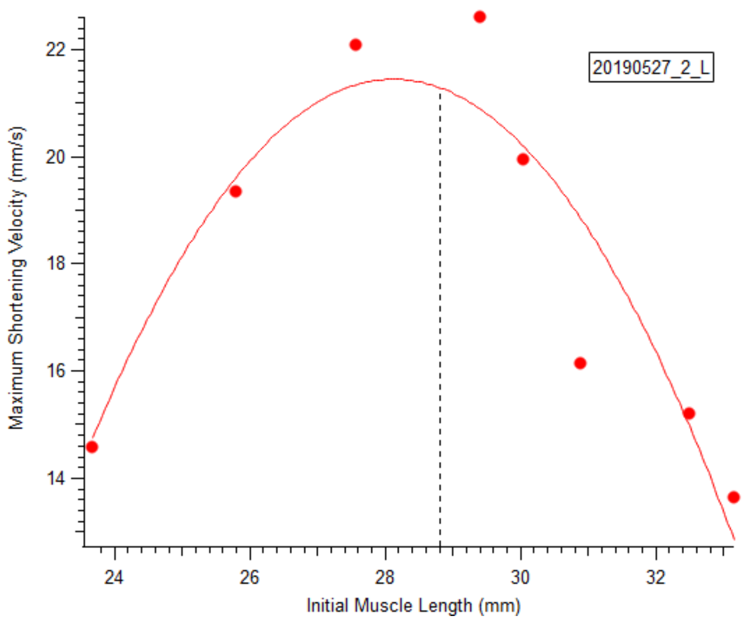

Figure 10. Example trace of maximum shortening velocities at different L_i values for a muscle in the "w/ tendon" condition. The initial length that resulted in L_0 for this muscle is marked with a dashed line.

DISCUSSION

The goal of this study was to evaluate how additional in-series compliance affects skeletal muscle L_0 in maximally activated contractions. Our findings show that L_0 decreases when series compliance is increased. Adding an artificial tendon to a muscle in the "w/ tendon" condition resulted in a decrease of 40.98 ± 8.47% ($p < 0.001$) and 10.74 ± 5.21% ($p < 0.01$) in P_0 and L_0, respectively, compared to the "muscle only" condition. This supports the hypothesis that muscle shortening affects L_0 and hence suggests that cross-bridge and sliding filament theories are subject to systematic errors, as they predict that L_0 is determined only by filament overlap. However, these results should be interpreted with caution because, while the force-length curves demonstrate a plateau, muscles with added series compliance in the "w/ tendon" condition could not be stretched to long enough lengths to see a substantial descending limb without causing significant muscle damage (**Figure 7**).

In an attempt to elucidate the effect of series compliance on L_0, fixed-end contractions were performed on muscles with parallel fiber orientation and minimal natural tendon. An artificial terminal tendon with considerable compliance was included or excluded to allow for the pronounced and carefully controlled modulation of series compliance. Muscles were activated and allowed to shorten against this artificial tendon, rather than us specifying the shortening velocity, amount of shortening, and work done.

Recent work found that no significant shift in L_0 occurred with additional series compliance in rat gastrocnemius muscles (MacDougall et al., 2020). However, some important differences exist between our experimental methods and those of MacDougall et al (2020) that may contribute to this discrepancy. Firstly, MacDougall et al. (2020) used the rat medial gastrocnemius muscle which has considerable naturally occurring series compliance, and added minimal additional series compliance. In comparison, we used a muscle with minimal series elasticity and added significant artificial series compliance. As a result, we saw much larger differences in amount of shortening with and without additional series compliance. MacDougall et al. (2020) reported shortening magnitudes of 1.40 ± 0.55 mm and 1.64 ± 0.61 mm for the low and high compliance conditions, respectively, while our "muscle only" condition had no shortening and "w/ tendon" contractions that resulted in L_0 had shortening magnitudes of 6.35 ± 1.86 mm. Further, the large difference in our additional series elastic component and resultant muscle shortening allowed for a substantial difference in work performed between our "w/ tendon" and "muscle only" conditions. The mean value for work in contractions that resulted in L_0 in the high compliance ("w/ tendon") condition was 5.97 ± 2.44 mJ, while there was minimal work in the low compliance ("muscle only") condition. This is a much greater difference than that reported by MacDougall et al (2020), with work values 3.64 ± 1.46 mJ and 4.1 ± 1.68 mJ for their low and high compliance conditions, respectively. The large difference in work and shifts in L_0 between our experiments and MacDougall et al. (2020) suggest that force and shortening may be important parameters for a possible mechanism that links shortening depression and shifts in L_0.

Since our "w/ tendon" muscles actively shortened before reaching isometry, and post-shortening isometric force was reduced compared to the "muscle only" condition, it is possible that a common mechanism is responsible for both shortening depression and the decrease in L_0 that was observed in our experiments. When muscle actively shortens before reaching isometry, P_0 decreases compared to a purely isometric contraction at the same reference length (Abbott & Aubert, 1952; Rassier & Herzog, 2004). Characteristics of shortening depression include: 1) it is long-lasting, 2) it disappears upon muscle deactivation, even if this deactivation is brief, 3) it increases proportionally with distance shortened, 4) it decreases with increased shortening velocity, 5) it increases with greater force during shortening, and, similarly 6) it increases with greater work during shortening (Abbott & Aubert, 1952; Granzier & Pollack, 1989; Herzog et al., 2000; Herzog & Leonard, 1997; Maréchal & Plaghki, 1979; Rassier & Herzog, 2004). Muscle shortening, and also the length at which isometry was reached in “w/ tendon” contractions, was set by muscle force and tendon properties, hence these lengths did not exactly match those in the “muscle only” condition, thus preventing us from precisely determining shortening depression in each contraction. However, we used the difference in P_0 between the two conditions as a proxy for shortening depression. Using our proxy method, the P_0 for “w/ tendon” experienced shortening depression of approximately 40.98 ± 8.47% compared to “muscle only” P_0. To understand how this drop in P_0 may be caused by shortening depression, the mechanisms of shortening depression will be explored further.

The proposed mechanisms behind shortening depression generally fall into one of three categories: 1) sarcomere length non-uniformity, 2) accumulation of fatigue by-products, or 3) inhibition of cross-bridge binding. Sarcomere length non-uniformity states that actively shortening muscles may have different sarcomere lengths due to instability that accompanies shortening from longer lengths on the descending limb of the force-length curve (Abbott & Aubert, 1952). On the other hand, the accumulation of fatigue by-products hypothesis suggests that the increase in the concentration of protons and inorganic phosphate after contraction and ATP consumption may cause the drop in active force with shortening (Granzier & Pollack, 1989). However, these mechanisms are unlikely to be the primary cause of shortening depression since sarcomeres are able to maintain stability on the descending limb and there is rapid recovery of force production following relaxation (Abbott & Aubert, 1952; Herzog & Leonard, 1997;

Joumaa et al., 2012; Rassier et al., 2003; Rassier & Herzog, 2004). The final mechanism commonly used to explain shortening depression is cross-bridge inhibition. This mechanism suggests that during active shortening, the likelihood of cross-bridge formation decreases due to the blocking of binding sites by titin (Rode et al., 2009) or that the strain-induced deformation of actin myofilaments results in decreased cross-bridge formation, and force, in both new regions of filament overlap (Maréchal & Plaghki, 1979) and the existing region of filament overlap (Joumaa et al., 2012). Of the mechanisms mentioned, cross-bridge inhibition seems to be the most likely mechanism of shortening depression that explains the shortening-dependent shift in L_0 that was observed in muscles with additional in-series compliance (Holt & Azizi, 2014; Holt & Williams, 2018).

The muscles in our “w/ tendon” experiments underwent fixed-end contractions and actively shortened against a compliant element before reaching isometry, so new regions of actin-myosin overlap were formed. Since myofilaments are strained in the newly formed region of overlap, it has been theorized that the likelihood of cross-bridge formation is altered (Corr & Herzog, 2016; Daniel et al., 1998; Herzog, 1998; Maréchal & Plaghki, 1979; Rassier & Herzog, 2004; Rode et al., 2009). Previous work proposes that regions of absolute and effective overlap exist that dictate the amount of isometric force produced by sarcomeres that actively shortened prior to becoming isometric (Holt & Williams, 2018). Absolute overlap refers to the entire region of myofilament overlap, including the original region of overlap and the new region of overlap after shortening, while effective overlap refers to the old region of overlap that existed prior to shortening and, therefore, where cross-bridge binding probability has likely been less affected (**Figures 11 & 12**). As active sarcomere shortening increases in fixed-end contractions, similar to our “w/ tendon” condition, the ratio of absolute to effective overlap is likely to increase. The new region of sarcomere overlap is predicted to produce less force due to inhibition of cross-bridge formation. Several factors, including the amount of additional in-series compliance and resultant shortening, may affect the ratio of absolute to effective overlap in muscles that are contracted with additional in-series compliance.

When two muscles, one with high compliance (**Figure 11a**), and one with low compliance (**Figure 11b**) contract and reach the same final length, they will theoretically have similar amounts of absolute sarcomere overlap. However, since the muscle in the high compliance condition actively shortens against a larger amount of series compliance before reaching isometry, it will have shortened more and cross-bridge inhibition may cause a smaller ratio of effective overlap to absolute overlap, resulting in a smaller amount of force produced. The events described here account for the decrease in force that accompanies shortening.

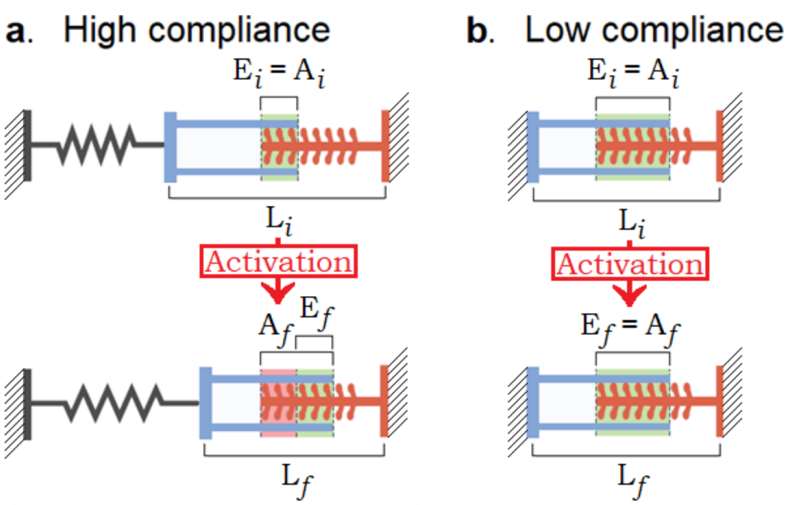

Figure 11. Proposed half-sarcomere mechanics in muscles actively shortening either with additional in-series compliance (**a**; high compliance "w/ tendon" condition) or without (**b**; low compliance "muscle only" condition), both having the same isometric length after activation (L_f). Since the isometric region of effective overlap (E_f) is less than the region of absolute overlap (A_f) in the high compliance, "w/ tendon" condition, the force is expected to be less than the low compliance, "muscle only" condition that has a much larger E_f region. Adapted from Holt & Williams (2018).

In addition to shortening under tension, a muscle with high compliance that contracts at the same starting length as a muscle with low compliance will shorten more and have a shorter L_f

(**Figure 12)**. As shortening increases, absolute overlap is likely to increase proportionally, but effective overlap stays approximately the same as it was before it was activated. This would result in shorter L_0 values as shortening increases. Theoretically, if binding sites are inhibited following shortening in “w/ tendon” contractions, a shorter L_0 will be reached than the L_0 of a purely isometric “muscle only” contraction due to a smaller ratio of effective overlap to absolute overlap (**Figure 11**). In addition to a decrease in force from shortening depression, each “w/ tendon” experiment experienced a decrease in L_0 compared to “muscle only” experiments, supporting that some mechanism of cross-bridge inhibition may have been present. We also propose that some aspect of this mechanism is present in the activation-dependent shift in L_0 that has previously been observed (Holt & Azizi, 2014; Holt & Williams, 2018).

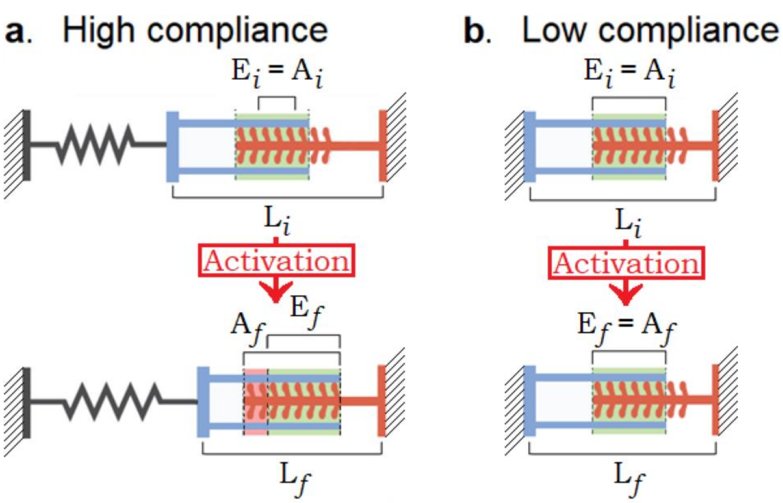

Figure 12. Proposed half-sarcomere mechanics in muscles actively shortening either with additional in-series compliance (**a**; high compliance “w/ tendon” condition) or without (**b**; low compliance “muscle only” condition), both having the same length before activation (L_i). Since the isometric region of effective overlap after contraction (E_f) is approximately the same as the region of absolute overlap after contraction (A_f) in the high compliance, “w/ tendon” condition, the expected force is expected to also be approximately the same as the low compliance, “muscle only” condition. However, since the high compliance “w/ tendon” muscle shortened before reaching L_f, it has a shorter final length. Adapted from Holt & Williams (2018).

When activation level is varied in a muscle with additional in-series compliance, the amount of shortening will vary with the most shortening occurring at higher activation levels. An increase in muscle shortening with increasing activation levels has been accompanied by a leftward shift in L_0 (Holt & Azizi, 2014; Holt & Williams, 2018). In our experiments, when "w/ tendon" muscles were stimulated maximally, they experienced more shortening than the "muscle only" condition that underwent purely isometric contractions. The "w/ tendon" experiments also resulted in a shorter L_0 that accompanied a decrease in P_0 compared to "muscle only" experiments. An important difference between our experiments and those of Holt & Azizi (2014) is that we maximally activated whole muscle while Holt & Azizi (2014) maximally activated subsets of motor units to achieve varying activation levels. Since changes in P_0 and L_0 occurred with maximally activated muscles in both experiments, this suggests that a purely calcium-independent mechanism that depends on shortening rather than changes in calcium level were at least partly responsible for these shifts. This presents a possible link between the shifts we observed and those of Holt & Azizi (2014). Though our experiments did not directly examine a mechanism for the shortening- or activation-dependent shifts in L_0, they may provide support for a proposed mechanism of strain-induced cross-bridge inhibition that links the two.

Other factors may also contribute to the observed shifts in L_0 and P_0. One possible factor is the increase in shortening velocity that occurs with shortening in the "w/ tendon" condition. With increasing shortening velocity, the force produced, and thus the work of a shortening contraction, will be reduced (Marechal and Plaghki, 1978). This would alter the amount of shortening depression which would likely also affect L_0. Another factor is that muscles may have reached their shortening end-point. With extreme shortening, sarcomeres may be unable to shorten further due to maximum myofilament overlap being reached. Many of the "w/ tendon" force-length curves aligned very closely with the trajectory of the ascending limb of the "muscle only" curves, supporting that this may have occurred. If this is the case, some mechanism related to thin filament regulatory proteins, myofilament geometry, or collision of thin filaments may contribute to the observed shifts in P_0 and L_0 (Bagni et al., 1990; Gordon et al., 1966; Konhilas et al., 2002; Rockenfeller et al., 2022). Further investigation into these mechanisms would be useful in determining the cause of the observed shift in L_0 with increased series compliance.

In conclusion, adding artificial series compliance to a muscle appears to result in a leftward shift in L_0 that accompanies a decrease in P_0, and the shift in L_0 may be caused by a combination of factors that includes shortening-induced cross-bridge inhibition. The findings presented here have physiological significance because most vertebrate skeletal muscles have varying amounts of compliant in-series tendons or aponeuroses that will change length and generate tension during contraction. This supports that tendons and muscle shortening are important inputs for muscle modelling and that muscle models that rely heavily on the purely isometric force-length relationship are subject to systematic errors.

REFERENCES

Abbott, B. C., & Aubert, X. M. (1952). The force exerted by active striated muscle during and after change of length. *The Journal of Physiology*, *117*, 77–86. https://doi.org/10.1113/jphysiol.1952.sp004733

Adrian, E. D., & Bronk, D. W. (1929). The discharge of impulses in motor nerve fibres. Part II. The frequency of discharge in reflex and voluntary contractions. *Journal of Physiology*, *Lxvii*(2), 119–151.

Bagni, M. A., Cecchi, G., & Colomo, F. (1990). Myofilament spacing and force generation in intact frog muscle fibres. *The Journal of Physiology*, *430*, 61–75. https://doi.org/10.1113/jphysiol.1990.sp018281

Brown, I. E., Cheng, E. J., & Loeb, G. E. (1999). Measured and modeled properties of mammalian skeletal muscle. II. The effects of stimulus frequency on force-length and force-velocity relationships. *Journal of Muscle Research and Cell Motility*, *20*(7), 627–643. https://doi.org/10.1023/A:1005585030764

Cavagna, G. A., Saibene, F. P., & Margaria, R. (1964). Mechanical work in running. *Journal of Applied Physiology*, *19*(2), 249–256. https://doi.org/10.1152/jappl.1964.19.2.249

Close, R. I. (1972). Sarcomere length and characteristics of isometric twitch contractions of frog sartorius muscle. *J. Physiol*, *220*, 745–762.

Corr, D. T., & Herzog, W. (2016). A cross-bridge based model of force depression: Can a single modification address both transient and steady-state behaviors? *Journal of Biomechanics*, *49*(5), 726–734. https://doi.org/10.1016/j.jbiomech.2016.02.005

Daniel, T. L., Trimble, A. C., & Chase, P. B. (1998). Compliant realignment of binding sites in muscle: Transient behavior and mechanical tuning. *Biophysical Journal*, *74*(4), 1611–1621. https://doi.org/10.1016/S0006-3495(98)77875-0

Dick, T. J. M., Biewener, A. A., & Wakeling, J. M. (2017). Comparison of human gastrocnemius forces predicted by Hill-type muscle models and estimated from ultrasound images. *Journal of Experimental Biology*, *220*(9), 1643–1653. https://doi.org/10.1242/jeb.154807

Duvall, M. M., Gifford, J. L., Amrein, M., & Herzog, W. (2013). Altered mechanical properties of titin immunoglobulin domain 27 in the presence of calcium. *European Biophysics Journal*, *42*(4), 301–307. https://doi.org/10.1007/s00249-012-0875-8

Edman, K. A. P., Caputo, C., & Lou, F. (1993). Depression of tetanic force induced by loaded shortening of frog muscle fibers. *J. Physiol*, *466*, 535–553.

Edman, K. A. P., Elzinga, G., & Noble, M. I. M. (1982). Residual force enhancement after stretch of contracting frog single muscle fibers. *Journal of General Physiology*, *80*(5), 769–784. https://doi.org/10.1085/jgp.80.5.769

Fuchs, F., & Smith, S. H. (2001). Calcium, cross-bridges, and the Frank-Starling relationship. *News in Physiological Sciences : An International Journal of Physiology Produced Jointly by the International Union of Physiological Sciences and the American Physiological Society*, *16*, 5–10. https://doi.org/10.1152/physiologyonline.2001.16.1.5

Goldman, Y. E., & Huxley, A. F. (1994). Actin compliance: Are you pulling my chain? *Biophysical Journal*, *67*(December), 2131–2133.

Gordon, A. M., Huxley, A. F., & Julian, F. J. (1966). The variation in isometric tension with sarcomere length in vertebrate muscle fibres. *J. Physiol*, *184*, 170–192.

Granzier & Pollack. (1989). Effect of active pre-shortening on isometric and isotonic performance of single frog muscle fibres. *J. Physiol*, *415*, 299–327.

Granzier, H. L., & Labeit, S. (2006). The giant muscle protein titin is an adjustable molecular spring. *Exercise and Sport Sciences Reviews*, *34*(2), 50–53. https://doi.org/10.1249/00003677-200604000-00002

Henneman, E, Somjen, G., & Carpenter, D. O. (1965). Excitability and inhibitability of motoneurons of different sizes. *Journal of Neurophysiology*, *28*(3), 599–620. https://doi.org/10.1152/jn.1965.28.3.599

Henneman, Elwood. (1957). Relation between size of neurons and their susceptibility to discharge. *Science*, *126*(3287), 1345–1347.

Henneman, Elwood, Somjen, G., & Carpenter, D. (1965). Funtional significance of cell size in spinal motoneurons. *J. Neurophysiol*, *28*, 560–580.

Herzog, J. A., Leonard, T. R., Jinha, A., & Herzog, W. (2014). Titin (Visco-) Elasticity in skeletal muscle myofibrils.pdf. *Molecular and Cellular Biocmechanics: MCB*, *11*(1), 1–17.

Herzog, W. (1998). History dependence of force production in skeletal muscle: A proposal for mechanisms. *Journal of Electromyography and Kinesiology*, *8*(2), 111–117. https://doi.org/10.1016/S1050-6411(97)00027-8

Herzog, W., Joumaa, V., & Leonard, T. R. (2010). The force-length relationship of mechanically isolated sarcomeres. *Advances in Experimental Medicine and Biology*, *682*, 141–161. https://doi.org/10.1007/978-1-4419-6366-6_8

Herzog, W., Lee, E. J., & Rassier, D. E. (2006). Residual force enhancement in skeletal muscle. *Journal of Physiology*, *574*(3), 635–642. https://doi.org/10.1113/jphysiol.2006.107748

Herzog, W., & Leonard, T. R. (1997). Depression of cat soleus forces following isokinetic shortening. *Journal of Biomechanics*, *30*(9), 865–872. https://doi.org/10.1016/S0021-9290(97)00046-8

Herzog, W., Leonard, T. R., & Wu, J. Z. (2000). The relationship between force depression following shortening and mechanical work in skeletal muscle. *Journal of Biomechanics*, *33*(6), 659–668. https://doi.org/10.1016/S0021-9290(00)00008-7

Hill, A. V. (1938). The heat of shortening and the dynamic constants of muscle. *Proceedings of the Royal Society of London. Series B - Biological Sciences*, *126*(843), 136–195. https://doi.org/10.1098/rspb.1938.0050

Hill, A. V. (1950). The dimensions of animals and their muscular dynamics. *Science Progress (1933-)*, *38*(150), 209–230. http://www.jstor.org/stable/43422833

Hodson-Tole, E. F., & Wakeling, J. M. (2009). Motor unit recruitment for dynamic tasks: Current understanding and future directions. *Journal of Comparative Physiology B: Biochemical, Systemic, and Environmental Physiology*, *179*(1), 57–66.

https://doi.org/10.1007/s00360-008-0289-1

Holt, N. C., & Azizi, E. (2014). What drives activation-dependent shifts in the force - Length curve? *Biology Letters*, *10*(9). https://doi.org/10.1098/rsbl.2014.0651

Holt, N. C., Roberts, T. J., & Askew, G. N. (2014). The energetic benefits of tendon springs in running: Is the reduction of muscle work important? *Journal of Experimental Biology*, *217*(24), 4365–4371. https://doi.org/10.1242/jeb.112813

Holt, N. C., Wakeling, J. M., & Biewener, A. A. (2014). The effect of fast and slow motor unit activation on whole-muscle mechanical performance: The size principle may not pose a mechanical paradox. *Proceedings of the Royal Society B: Biological Sciences*, *281*(1783), 2–7. https://doi.org/10.1098/rspb.2014.0002

Holt, N. C., & Williams, C. D. (2018). Can strain dependent inhibition of cross-bridge binding explain shifts in optimum muscle length? *Integrative and Comparative Biology*, *58*(2), 174–185. https://doi.org/10.1093/icb/icy050

Hutchinson, J. R., Rankin, J. W., Rubenson, J., Rosenbluth, K. H., Siston, R. A., & Delp, S. L. (2015). Musculoskeletal modelling of an ostrich (Struthio camelus) pelvic limb: influence of limb orientation on muscular capacity during locomotion. *PeerJ*, *3*, e1001. https://doi.org/10.7717/peerj.1001

Huxley, A. F. (1957). Muscle structure and theories of contraction. *Progress in Biophysics and Biophysical Chemistry*, *7*, 255–318.

Huxley, A. F. (1974). Muscular Contraction. *J Physiol*, *243*(1), 1–43.

Huxley, A. F., & Niedergerke, R. (1954). *Structural Changes in Muscle During Contraction.pdf* (pp. 971–973).

Huxley, A. F., & Simmons, R. M. (1971). Proposed mechanism of force generation in striated muscle. *Nature*, *233*(5321), 533–538. https://doi.org/10.1038/233533a0

Huxley, H. E. (1969). The mechanism of muscular contraction. *Science (New York, N.Y.)*, *164*(3886), 1356–1365. https://doi.org/10.1126/science.164.3886.1356

Huxley, H. E., & Hanson, J. (1954). Changes in the Cross-Striations of Muscle during Contraction and Stretch and their Structural Interpretation. *Nature*, *173*(4412), 973–976. https://doi.org/10.1038/173973a0

Huxley, H. E., Stewart, A., Sosa, H., & Irving, T. (1994). X-ray diffraction measurements of the extensibility of actin and myosin filaments in contracting muscle. *Biophysical Journal*, *67*(6), 2411–2421. https://doi.org/10.1016/S0006-3495(94)80728-3

Joumaa, V., MacIntosh, B., & Herzog, W. (2012). New insights into force depression in skeletal muscle. *Journal of Experimental Biology*, *215*(12), 2135–2140. https://doi.org/10.1242/jeb.060863

Joumaa, V., Rassier, D. E., Leonard, T. R., & Herzog, W. (2008). The origin of passive force enhancement in skeletal muscle. *American Journal of Physiology - Cell Physiology*, *294*(1), 74–78. https://doi.org/10.1152/ajpcell.00218.2007

Kargo, W. J., & Rome, L. C. (2002). Functional morphology of proximal hindlimb muscles in the frog Rana pipiens. *Journal of Experimental Biology*, *205*(14), 1987–2004.

https://doi.org/10.1242/jeb.205.14.1987

Konhilas, J. P., Irving, T. C., & de Tombe, P. P. (2002). Length-dependent activation in three striated muscle types of the rat. *The Journal of Physiology*, *544*(1), 225–236. https://doi.org/https://doi.org/10.1113/jphysiol.2002.024505

Labeit, D., Watanabe, K., Witt, C., Fujita, H., Wu, Y., Lahmers, S., Funck, T., Labeit, S., & Granzier, H. (2003). Calcium-dependent molecular spring elements in the giant protein titin. *Proceedings of the National Academy of Sciences of the United States of America*, *100*(23), 13716–13721. https://doi.org/10.1073/pnas.2235652100

Liddell, E. G. T., & Sherrington, O. M. (1925). Recruitment and some other features of reflex inhibition. *Proceedings of the Royal Society B: Biological Sciences*, *97*(686), 488–518. https://doi.org/10.1098/rspb.1925.0016

Lindstedt, S. L. (2016). Skeletal muscle tissue in movement and health: positives and negatives. *Journal of Experimental Biology*, *219*(2), 183–188. https://doi.org/10.1242/jeb.124297

MacDougall, K., Kristensen, A., & MacIntosh, B. (2020). Additional in-series compliance does not affect the length dependence of activation in rat medial gastrocnemius. *Experimental Physiology*, *105*, 1907–1917.

MacIntosh, B. R. (2017). Recent developments in understanding the length dependence of contractile response of skeletal muscle. *European Journal of Applied Physiology*, *117*(6), 1059–1071. https://doi.org/10.1007/s00421-017-3591-3

Maréchal, G., & Plaghki, L. (1979). The deficit of the isometric tetanic tension redeveloped after a release of frog muscle at a constant velocity. *Journal of General Physiology*, *73*(4), 453–467. https://doi.org/10.1085/jgp.73.4.453

Mayfield, D., Launikonis, B., Cresswell, A., & Lichtwark, G. (2016). Additional in-series compliance reduces muscle force summation and alters the time course of force relaxation during fixed-end contractions. *Journal of Experimental Biology*, *219*(22), 3587–3596. https://doi.org/10.1242/jeb.143123

Minozzo, F. C., & de Lira, C. A. B. (2013). Muscle residual force enhancement: A brief review. *Clinics*, *68*(2), 269–274. https://doi.org/10.6061/clinics/2013(02)R01

Nishikawa, K. (2016). Eccentric contraction: Unraveling mechanisms of force enhancement and energy conservation. *Journal of Experimental Biology*, *219*(2), 189–196. https://doi.org/10.1242/jeb.124057

Nishikawa, K., Monroy, J. A., Uyeno, T. E., Yeo, S. H., Pai, D. K., & Lindstedt, S. L. (2012). Is titin a “winding filament”? A new twist on muscle contraction. *Proceedings of the Royal Society B: Biological Sciences*, *279*(1730), 981–990. https://doi.org/10.1098/rspb.2011.1304

O’Neill, M. C., Lee, L. F., Larson, S. G., Demes, B., Stern, J. T., & Umberger, B. R. (2013). A three-dimensional musculoskeletal model of the chimpanzee (Pan troglodytes) pelvis and hind limb. *Journal of Experimental Biology*, *216*(19), 3709–3723. https://doi.org/10.1242/jeb.079665

Perreault, E. J., Heckman, C. J., & Sandercock, T. G. (2003). Hill muscle model errors during movement are greatest within the physiologically relevant range of motor unit firing rates.

Journal of Biomechanics, *36*(2), 211–218. https://doi.org/10.1016/S0021-9290(02)00332-9

Rack, P. M. H., & Westbury, D. R. (1969). The effects of length and stimulus rate on tension in the isometric cat soleus muscle. *The Journal of Physiology*, *204*(2), 443–460. https://doi.org/10.1113/jphysiol.1969.sp008923

Randall, D. J., Burggren, W. W., & French, K. A. (1997). *Eckert Animal Physiology: Mechanisms and Adaptations*.

Rassier, D. E., & Herzog, W. (2004). Considerations on the history dependence of muscle contraction. *Journal of Applied Physiology*, *96*(2), 419–427. https://doi.org/10.1152/japplphysiol.00653.2003

Rassier, D. E., Herzog, W., & Pollack, G. H. (2003). Stretch-induced force enhancement and stability of skeletal muscle myofibrils. *Advances in Experimental Medicine and Biology*, *538*, 501–515; discussion 515. https://doi.org/10.1007/978-1-4419-9029-7_45

Rassier, D. E., MacIntosh, B. R., & Herzog, W. (1999). Length dependence of active force production in skeletal muscle. *Journal of Applied Physiology*, *86*(5), 1445–1457. https://doi.org/10.1109/islc.2004.1382723

Roberts, T. J. (2016). Contribution of elastic tissues to the mechanics and energetics of muscle function during movement. *Journal of Experimental Biology*, *219*(2), 266–275. https://doi.org/10.1242/jeb.124446

Rockenfeller, R., Günther, M., & Hooper, S. L. (2022). Muscle active force-length curve explained by an electrophysical model of interfilament spacing. *Biophysical Journal*, *121*(10), 1823–1855. https://doi.org/10.1016/j.bpj.2022.04.019

Rode, C., Siebert, T., & Blickhan, R. (2009). Titin-induced force enhancement and force depression: A “sticky-spring” mechanism in muscle contractions? *Journal of Theoretical Biology*, *259*(2), 350–360. https://doi.org/10.1016/j.jtbi.2009.03.015

Rode, C., Siebert, T., Herzog, W., & Blickhan, R. (2009). The effects of parallel and series elastic components on the active cat soleus force-length relationship. *Journal of Mechanics in Medicine and Biology*, *9*(1), 105–122. https://doi.org/10.1142/S0219519409002870

Sandow, A. (1952). Excitation-contraction coupling in muscular response. *The Yale Journal of Biology and Medicine*, *25*(3), 176–201.

Stephenson, D. G., & Wendt, I. R. (1984). Length dependence of changes in sarcoplasmic calcium concentration and myofibrillar calcium sensitivity in striated muscle fibres. *Journal of Muscle Research and Cell Motility*, *5*(3), 243–272. https://doi.org/10.1007/BF00713107

Strojnik, V. (1995). Muscle activation level during maximal voluntary effort. *European Journal of Applied Physiology and Occupational Physiology*, *72*(1), 144–149. https://doi.org/10.1007/BF00964129

Wakabayashi, K., Sugimoto, Y., Tanaka, H., Ueno, Y., Takezawa, Y., & Amemiya, Y. (1994). X-ray diffraction evidence for the extensibility of actin and myosin filaments during muscle contraction. *Biophysical Journal*, *67*(6), 2422–2435. https://doi.org/10.1016/S0006-3495(94)80729-5

Winters, J. M. (1990). Hill-Based Muscle Models: A Systems Engineering Perspective. In J. M.

Winters & S. L.-Y. Woo (Eds.), *Multiple Muscle Systems: Biomechanics and Movement Organization* (pp. 69–93). Springer New York. https://doi.org/10.1007/978-1-4613-9030-5_5

Yang, Z., Stull, J. T., Levine, R. J., & Sweeney, H. L. (1998). Changes in interfilament spacing mimic the effects of myosin regulatory light chain phosphorylation in rabbit psoas fibers. *Journal of Structural Biology*, *122*(1–2), 139–148. https://doi.org/10.1006/jsbi.1998.3979

Zajac, F. E. (1989). Muscle and tendon: properties, models, scaling, and application to biomechanics and motor control. In *Critical reviews in biomedical engineering* (Vol. 17, Issue 4, pp. 359–411).

FIGURES

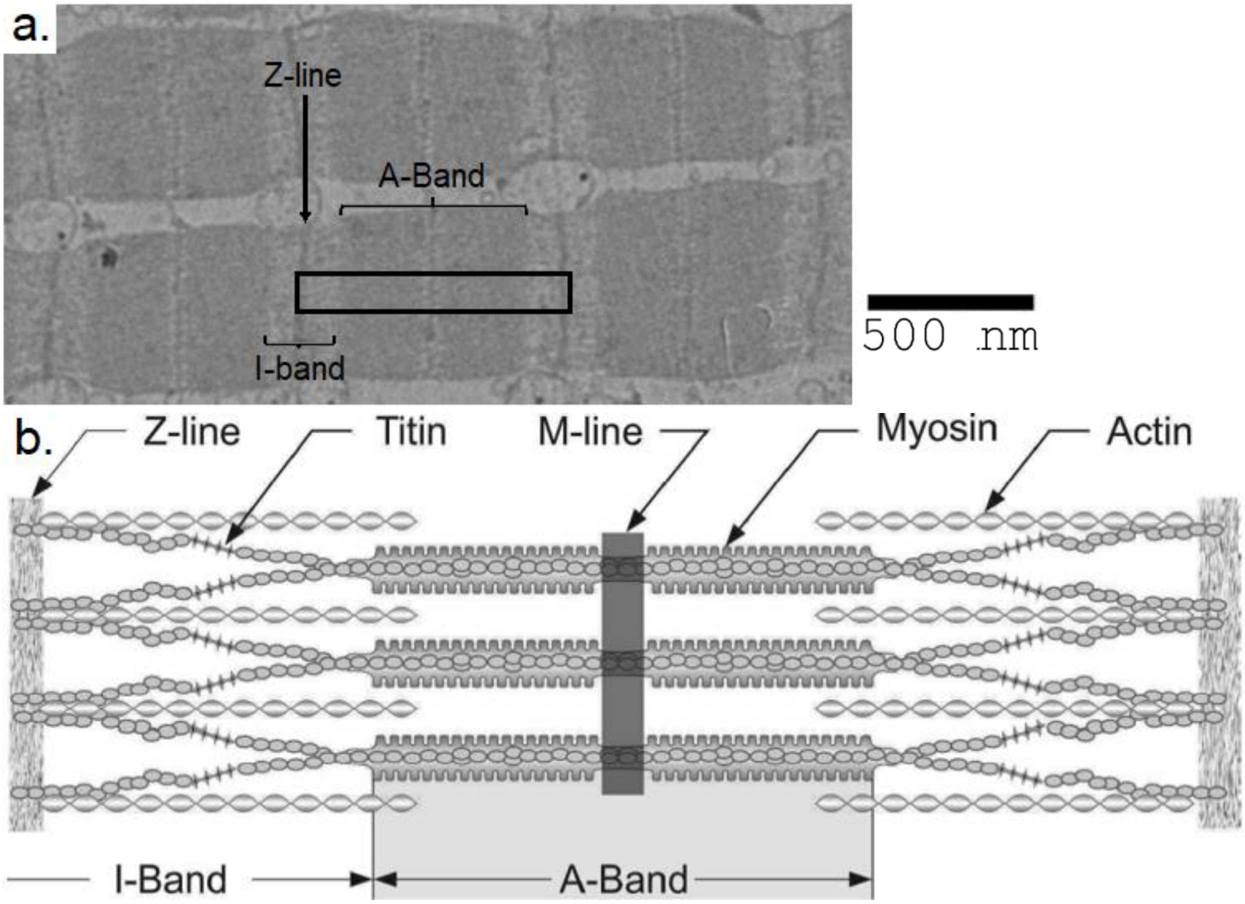

Figure 1. Transmission electron micrograph (1a) and diagram of the rectangular cutout from 1a showing structural landmarks within a sarcomere (1b). Figure 1a shows two muscle fibers in parallel to one another. Figure 1b shows three sarcomeres in parallel (Figure 1a imaged at Northern Arizona University Imaging Histology Core Facility; Figure 1b adapted from Granzier & Labeit, 2006; J. A. Herzog et al., 2014).

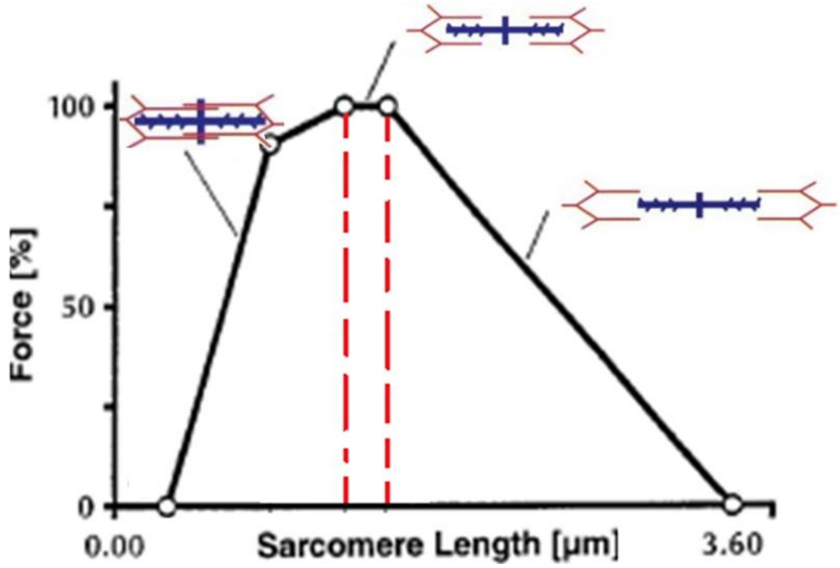

Figure 2. Muscle force-length relationship and sarcomere length (adapted from Gordon et al., 1966).

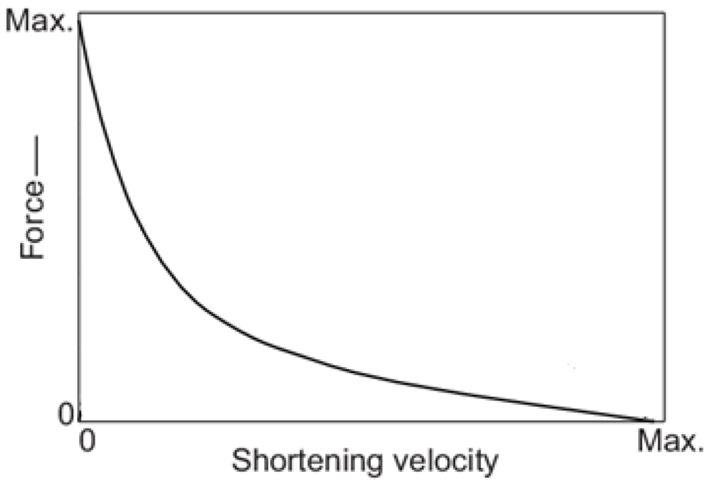

Figure 3. The magnitude of force that a muscle can produce decreases as shortening velocity increases (from Lindstedt, 2016; adapted from Hill, 1950)

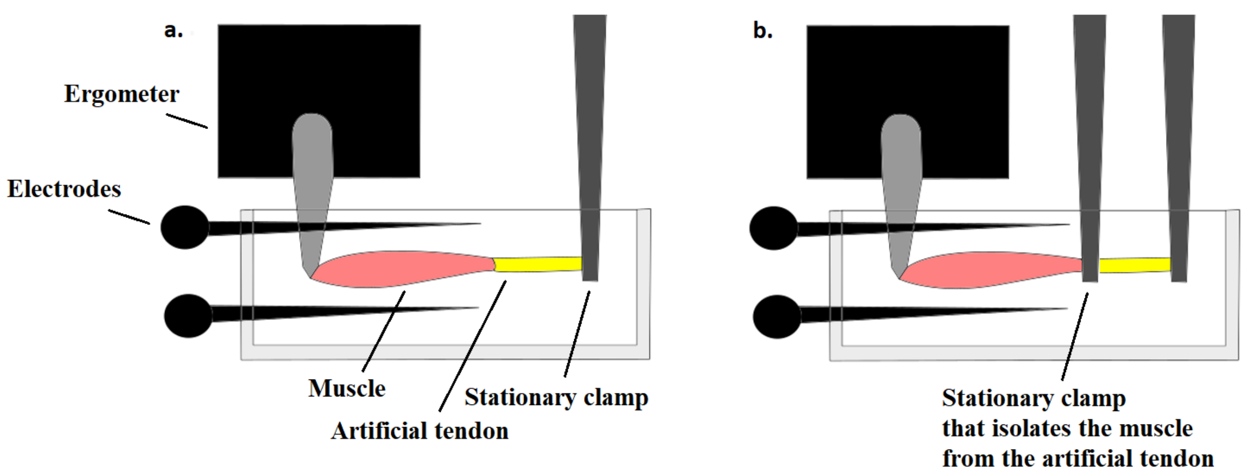

Figure 4. Schematic showing "w/ tendon" (a) and "muscle only" (b) conditions. In both conditions, MTU

or muscle is attached to an ergometer on the left and static anchor on the right. In the "muscle only" condition, an additional stationary clamp is used to isolate the muscle from the artificial tendon. Muscle is submerged in isotonic Ringer's solution and is surrounded by electrodes that deliver stimulation.

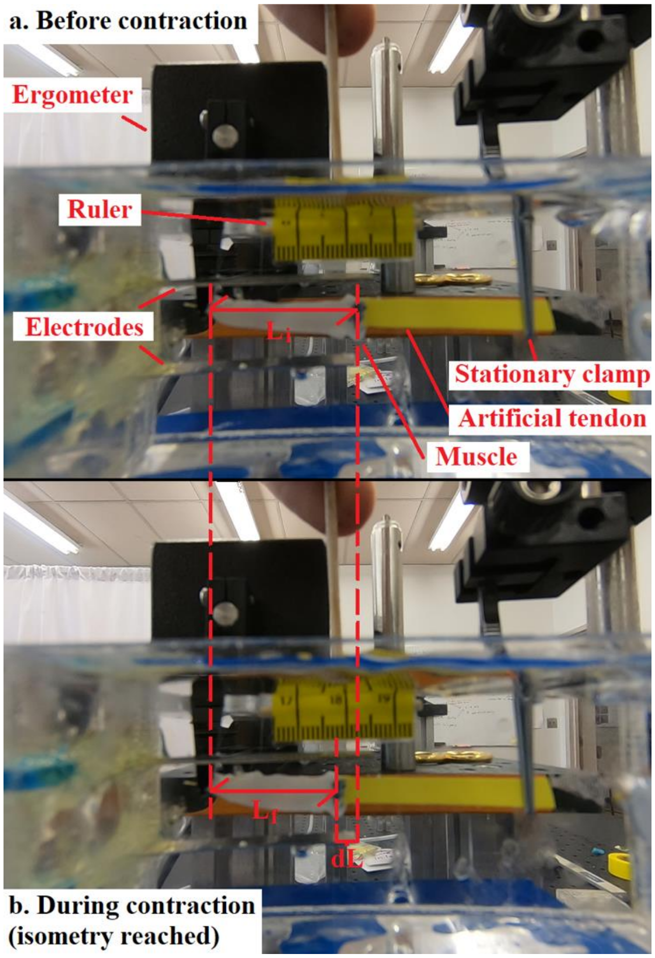

Figure 5. An example "w/ tendon" contraction. The top screenshot (a) shows the muscle before activation at its initial length (L_i). The lower screenshot (b) shows the active muscle at its shortened length (L_f) where isometry is reached. The amount of shortening is shown as the change in length (dL). ImageJ was used for frame-by-frame tracking of two terminal points at opposite ends of the muscle. A small ruler was submerged and used to convert between pixels and millimeters.

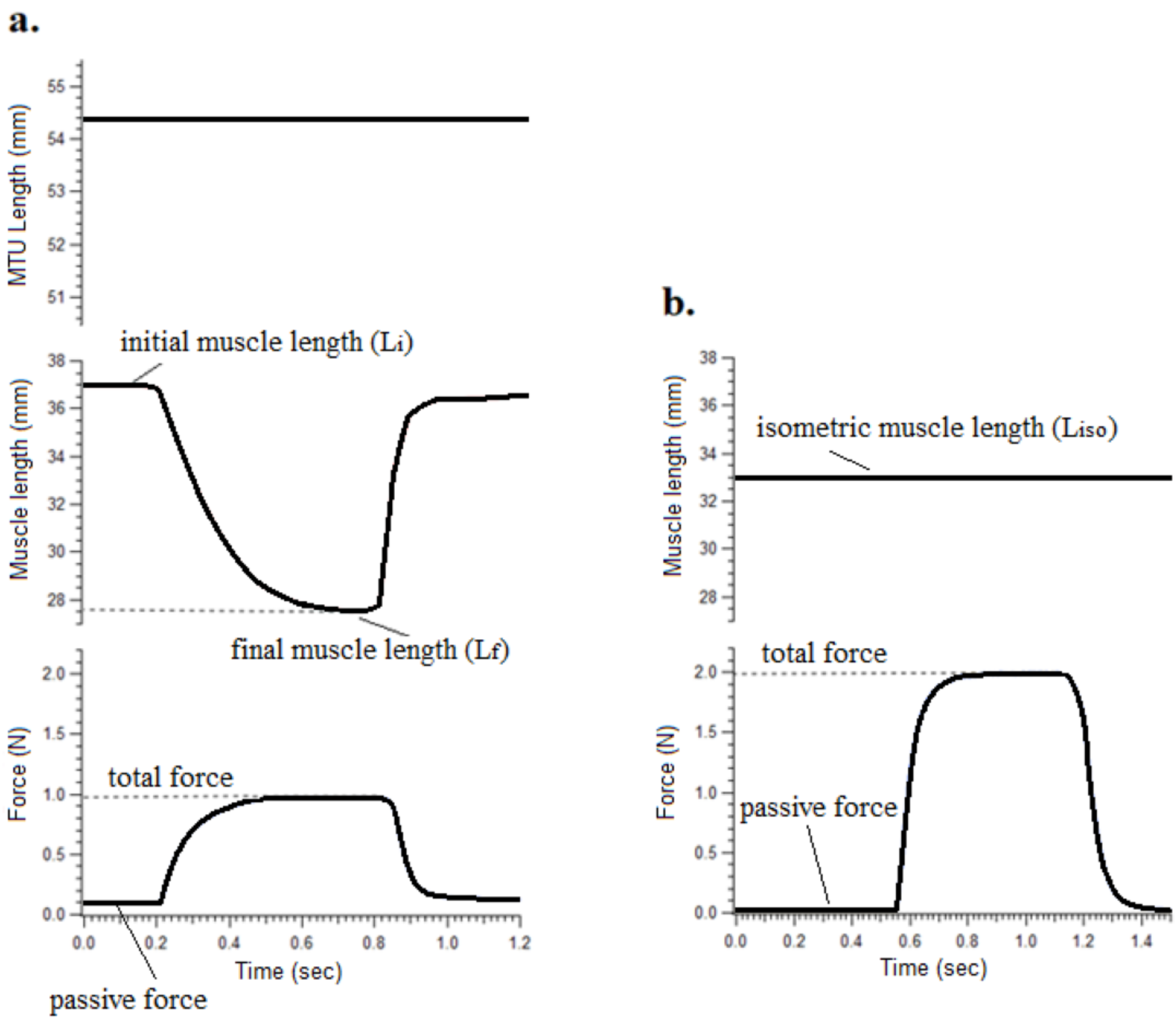

Figure 6. "W/ tendon" (a) and "muscle only" (b) total force and length traces for one contraction of each type. Dashed lines represent the total force and length values that were gathered at isometry. Total force and passive force values were used to find active force, and active force and length values were used to construct a force-length curve (**Figure 7**; open points).

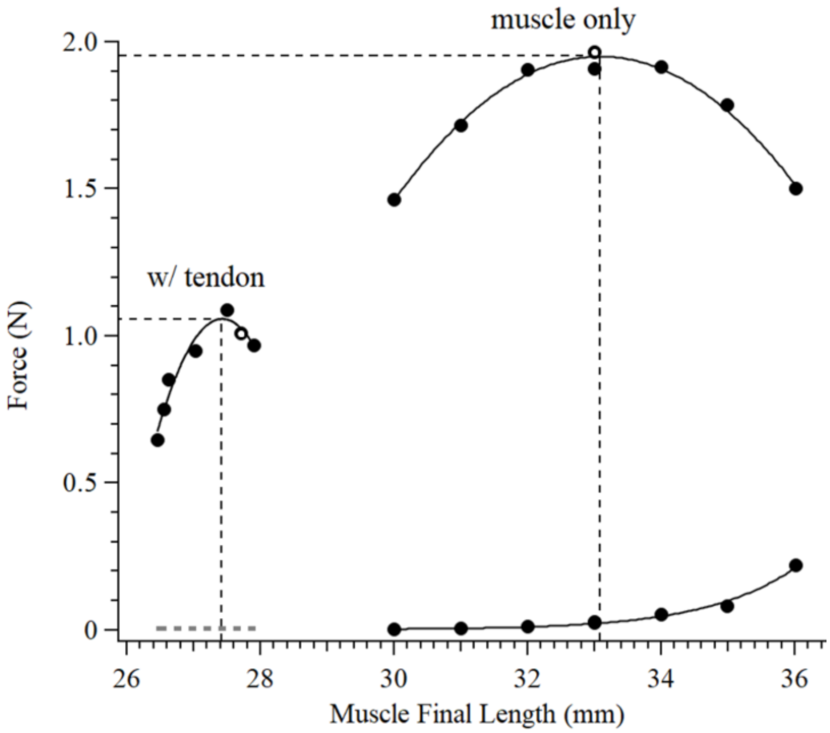

Figure 7. Force-length summary traces for “w/ tendon” and “muscle only” contractions on the same muscle. Upper curves are active force at isometry, lower curves are passive force pre-contraction. Since passive force is a function of the force of both the muscle and tendon in the “w/ tendon” condition, the “muscle only” passive force was extrapolated to the “w/ tendon” shortened lengths (dashed grey line). Open points are from the force-length traces in **Figure 6**.

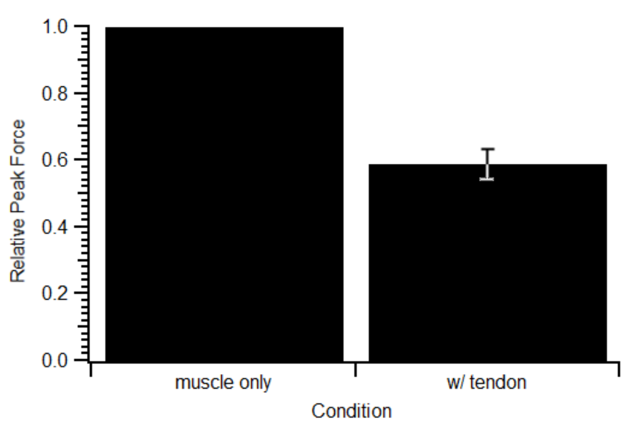

Figure 8. The “w/ tendon” condition experienced a decrease in both P_0 and L_0 compared to muscle only contractions. Relative values are calculated as the average “muscle only” value divided by “w/ tendon” value ± SD.

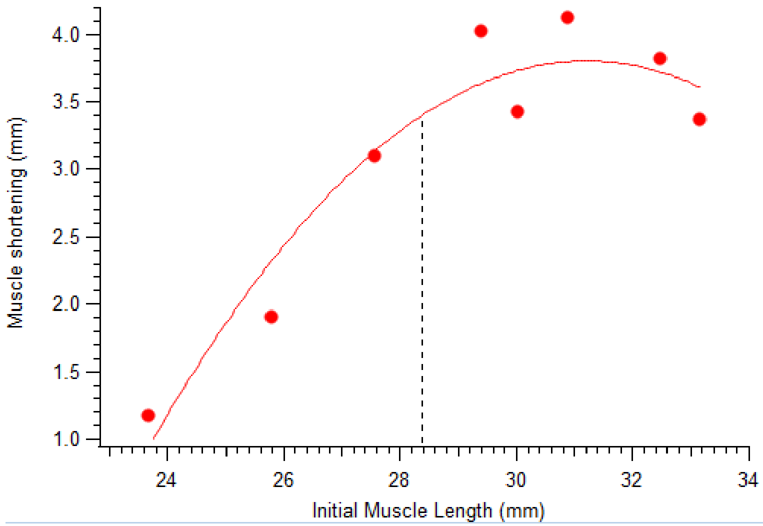

Figure 9. Graph showing the relationship between the amount of muscle shortening and the initial muscle length for one muscle (before the muscle was contracted). Dashed line represents L_0 for this muscle.

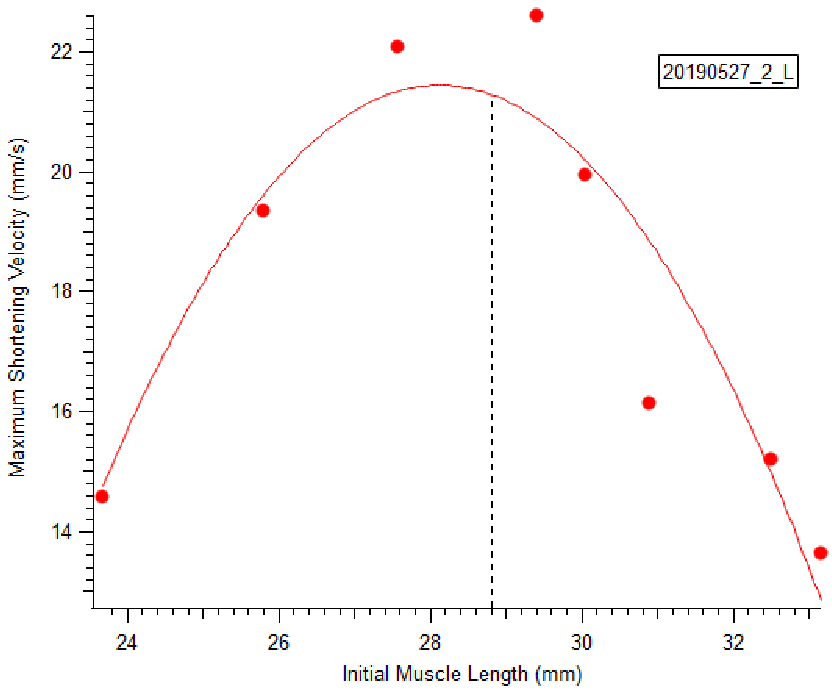

Figure 10. Example trace of maximum shortening velocities at different L_i values for a muscle in the "w/ tendon" condition. Optimum length for this muscle is marked with a dashed line.

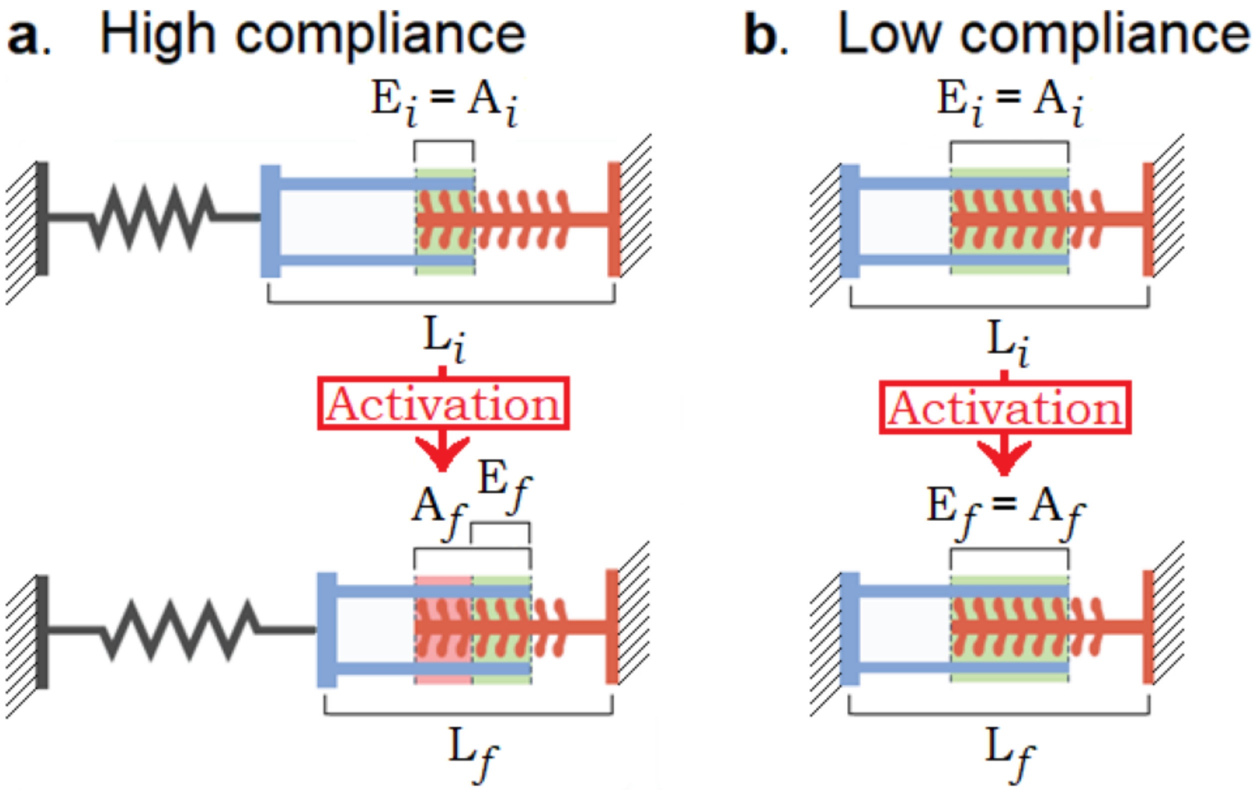

Figure 11. Proposed half-sarcomere mechanics in muscles actively shortening either with additional in-series compliance (**a**; high compliance "w/ tendon" condition) or without (**b**; low compliance "muscle only" condition), both having the same isometric length after activation (L_f). Since the isometric region of effective overlap (E_f) is less than the region of absolute overlap (A_f) in the high compliance, "w/ tendon" condition, the expected force is expected to be less than the low compliance, "muscle only" condition that has a much larger E_f region. Adapted from Holt & Williams (2018).

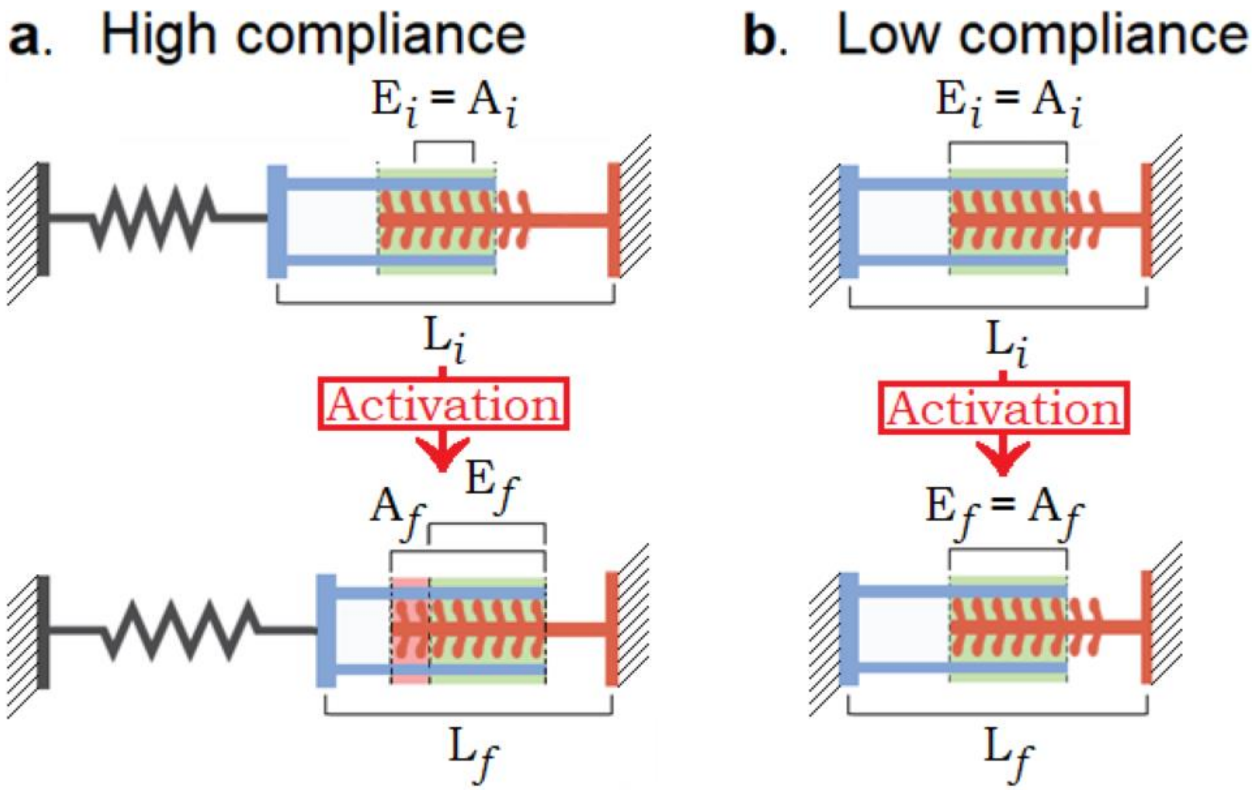

Figure 12. Proposed half-sarcomere mechanics in muscles actively shortening either with additional in-series compliance (**a**; high compliance "w/ tendon" condition) or without (**b**; low compliance "muscle only" condition), both having the same length before activation (L_i). Since the isometric region of effective overlap after contraction (E_f) is approximately the same as the region of absolute overlap after contraction (A_f) in the high compliance, "w/ tendon" condition, the expected force is expected to also be approximately the same as the low compliance, "muscle only" condition. However, since the high compliance "w/ tendon" muscle shortened before reaching L_f, it has a shorter final length. Adapted from Holt & Williams (2018).